TWO METHODS TO MEASURE THE $e^{\pm}$ POLARIZATION AT PEP

U. Camerini, D. B. Cline, J. G. Learned, A. K. Mann,
L. K. Resvanis, and P. J. Wanderer

ABSTRACT

Backward Compton scattering of circularly polarized photons from an $e^{\pm}$ beam can be used to measure the polarization of that beam. We describe a simple, compact, fast monitor that measures the beam polarization at P.E.P. by scattering a laser beam off the $e^{\pm}$ bunches and detecting the backscattered photons. We also present graphs of how the $\frac{d\sigma}{d\Omega}$ of the electromagnetic processes $e^+e^- \to e^+e^-, \mu^+\mu^-, \gamma\gamma$ is modified by the transverse polarization of the initial state particles.

The cross section for Compton scattering of polarized photons on polarized electrons has been calculated by Lipps and Tolhoek.[1,2,3] The cross section for backward Compton scattering of circularly polarized photons on polarized electrons is, in the lab frame,

$$\frac{d^2\sigma}{d\rho d\phi} = \frac{d^2\sigma_o}{d\rho d\phi} \pm P_{\ell} P_{\gamma} \left(\cos\psi \frac{d^2\sigma_1}{d\rho d\phi} + \sin\psi\cos\phi \frac{d^2\sigma_2}{d\rho d\phi} \right) \quad (1)$$

where $\rho = K_f/K_{f_{max}}$ (energy of back scattered photon)/(maximum energy)

$K_{f_{max}} = 4a\gamma^2 K_i$

K_i = incident photon energy

$a = 1/(1 + 4\gamma K_i/m)$

ϕ = angle between the scattering plane and the plane containing the e^- momentum and e polarization vector.

ψ = angle between the beam direction and the electron spin in the electron rest frame.

$$\frac{d^2\sigma_o}{d\rho d\phi} = r_o^2 a \left[\frac{\rho^2(1-a)^2}{1-\rho(1-a)} + 1 + \left(\frac{1-\rho(1+a)}{1-\rho(1-a)} \right)^2 \right]$$

$$\frac{d^2\sigma_1}{d\rho d\phi} = r_o^2 a \left[\left(1-\rho(1-a)\right) \left(1 - 1/[i-\rho(1-a)]^2\right) \right]$$

$$\frac{d^2\sigma_2}{d\rho d\phi} = r_o^2 a \left[\rho(1-a)\sqrt{4\, a\, \rho(1-\rho)}/[1-\rho(1-a)] \right]$$

For transversely polarized electrons the term in σ_1 is zero and the term in σ_2 represents the azimuthal asymmetry of the back scattered photons.

The lab angle θ between the incident and the back scattered photon is

$$\theta \simeq \frac{1}{\gamma}\sqrt{(1-\rho)/(a\rho)} \quad .$$

$$\text{Define} \quad s_o = \int \frac{d^2\sigma_o}{d\rho d\phi}\,, \quad s_1 = \int \frac{d^2\sigma_1}{d\rho d\phi}\,, \quad s_2 = \int \frac{d^2\sigma_2}{d\rho d\phi}\,.$$

For the case of transversely polarized $e^{\pm}$ call $\Sigma_{up} = s_o + s_2$, $\Sigma_{down} = s_o - s_2$. The asymmetry can be defined as

$$\frac{\Sigma_{up} - \Sigma_{down}}{(\Sigma_{up} + \Sigma_{down})/\sigma} = \frac{2s_2}{s_o} = A\,.$$

An alternate method of measuring the electron polarization is to use two counters one above and one below the beam plane, and to observe the change in counting rate (Σ) that occurs when the (circular) polarization of the incident photons is reversed.

This "modulation", M, of the counting rate is in the preceding ideal case of an infinitely thin electron beam and of two infinite counters identical with the asymmetry A,

$$2\,\frac{\Sigma^{\circlearrowright} - \Sigma^{\circlearrowleft}}{\Sigma^{\circlearrowright} + \Sigma^{\circlearrowleft}} = \frac{2s_2}{s_o}\,.$$

In the case of longitudinal polarization of the $e^{\pm}$ there is no up-down asymmetry but there is a modulation due to s_1. Note also that the energy dependence of s_1 and s_2 is different.

Experimental Arrangement

The experimental arrangement envisaged is shown schematically in Fig. 1: a linearly polarized laser beam is changed into a circularly polarized beam by means of a quarter wave plate, or similar optical device.

The device is capable of producing both polarization states (right and left circularly polarized) or to leave the beam with its original linear polarization. The laser beam is then reflected by a system of mirrors, and forms a very small angle with the electron beam at the interaction region.

The counters will be mounted so that the assembly can be rotated about a horizontal axis (substituting No. 1 for No. 2) and moved in a vertical direction for centering on the beam plane. Various types of counters can be used: e.g., glass Cerenkov or NaI counters for total absorption of the γ rays with the possible addition of a γ converter and a proportional chamber to count the number of converted γ rays.

Some of the experimental specifications are:

- The laser must be stable in output power to a few percent and should have a short wavelength and reasonably high power.
- A lens will focus the laser beam.
- The quarter wave plate must be stable and rotatable and the photon polarization state monitorable.
- The mirror system and windows must not change the polarization of the beam.

The counters must be stable, efficient and as symmetrically constructed as possible. By changing counter positions and laser polarization we can detect counter asymmetries and efficiencies as long as the electron beam and laser system are sufficiently stable over the measurement interval.

In order to estimate the experimental asymmetry we have integrated numerically the cross sections $s_0' = \int(d^2\sigma_0/d\rho d\phi)$ and $s_2' = \int(d^2\sigma_2/d\rho d\phi)$ over the surfaces of the counters for various values of the physical parameters involved. s_0' and s_2' are different from s_0 and s_2 in that the former quantities involve integrals over the counters (which may be arbitrarily positioned) rather than integrals over the half planes above and below the electron beam-line. The parameters to be considered are:

λ = wavelength of the laser

E = energy of the electron beam

W = beam vertical thickness

h = distance between <u>edge</u> of counter and beam plane (call it offset)

d = distance from counters to the photon-electron intersection region.

The normalized beam density function for the electron beam is taken as

$$D(z,z') = \frac{\beta}{2\pi W^2}\, e^{-\frac{[(1+\alpha^2)]z^2 + 2\alpha\beta z z' + \beta^2 z'^2}{2W^2}} \qquad (2)$$

where z = the distance above the beam axis and

z' = the slope of the trajectory.

The number of counts per bucket will be

$$N = \frac{2n_1 n_2 \Sigma L A_3}{A_1 A_2 C}$$

where

n_1 = number of electrons in bucket

Σ = effective cross section into counter (m^2), i.e., $s'_o + s'_2$ or $s'_o - s'_2$.

L = length of interaction region (m)

n_2 = photons per second

$= s \times 10^{24} \times P_{watts} \times \lambda_m$

A_1 = cross sectional area of laser beam (m^2)

A_2 = cross sectional area of electron beam (m^2)

A_3 = area in m^2 of the intersection $A_1 \cap A_2$

λ_m = laser wavelength (meters)

P = CW laser power (or instantaneous power for pulsed laser)

We conclude that the simultaneous use of asymmetry and modulation measurements are a strong tool in detecting the transverse polarization of electrons at PEP.

A large number of cross checks can be made by rotating the counters and by switching from circularly polarized to linearly polarized photons.

1. With linearly polarized light the asymmetry $A = 0$ for both counter positions.
2. With circularly polarized light the modulations M_1 and M_2 must be equal to each other and equal to the asymmetry A.
3. A change in the asymmetry A without a large accompanying change in the modulation indicates the electron beam has moved vertically.
4. It must be noted here that measurements of the background alone can be made by switching the laser beam off.

The detector should be placed in such a distance away from the scattering area as to give enough flight path so that if for instance the photon helicity is such as most scattered photons go upwards, then photons scattered upwards by electrons in the lower part of the beam should be above the beam plane at the detection point.

Obviously the synchrotron radiation is strongly dependent on the radius of curvature. The critical energy, $\epsilon_c = 2218 \times \frac{E^3}{R_{magnetic}} \frac{m}{GeV^3}$ ev and number of photons /sec/ev/mA/mrad $\propto \frac{1}{R^2_{magnetic}}$.

So, if instead of the last 2-3 cm of a regular bending magnet one had some kind of a tapered magnet where the magnetic radius would be much larger but the total $\int B \cdot d\ell$ stayed the same as not to affect the beam optics the synchrotron radiation emitted there could be a few orders of magnitude less than in the regular bending magnet. One should also keep in mind that approximately 1 rad. length of Pb will attenuate the synchrotron radiation by a factor of 10^4.

In Figures 2, 3, 4 and 5 we show the backscattered photon rates from a single bunch, the corresponding modulation (assuming maximal polarization) and time needed in order to measure the polarization of a single bunch with an accuracy of 10% as functions of the distance of the counters from the beam orbit plane, we have assumed zero background. These calculations were made for a beam energy of 15 GeV and a laser of 20 W, 5140 Å, 0.1 cm^2 laser area. Only photons with energy $0.2\ E_{max} \leq E_f \leq 0.8\ E_{max}$ were counted where at 15 GeV, $E_{max} = 5.3$ GeV for this laser, an interaction (scattering) length of the laser photons with the electrons of $\sim$12 cm was used. These rates could be much higher if a more powerful laser was used, e.g., lasers with 50 W instantaneous power and a repetition rate equal to the machine orbital frequency are available today. We have used the values for the vertical beta function β_y, its divergence α_y and the standard deviation of the vertical beam profile σ_y that the PEP designers consider realistic. The calculations were made for typical values of 20 m, 50 m, 100m of the distance of the scattering area to the detector. These distances and the angles involved are such that one can use the existing tunnel.

Beam gas bremsstrahlung for a pressure of 6×10^{-9} Torr of CO + 6×10^{-9} Torr of H_2 and for a source length of ~ 10 cm would produce a rate of 2-3 KHz which is comparable to the signal. If one scatters the laser off the e^- in the straight insertion, the pressure will be less by at least a factor of 10 but then in order to prevent the detector from getting blasted by the beam gas bremsstrahlung generated in the whole straight insertion (~ 130 m long) we should use a beam bump that would divert the beam at the scattering area by a few mrad. Figure 6 shows the factor that one has to multiply the time needed for the measurement of the polarization to 10% when there is no background for the corresponding signal/noise ratio.

Concluding, we believe that the "laser monitor" will enable us to measure accurately the polarization in a few minutes. Although there is clearly an optimum point in the PEP lattice to scatter the laser and correspondingly an optimum distance from the scattering area to the detector, given reasonable points for the scattering the time needed to complete the measurements varies only by factors of 2 or 3 so other considerations should play just as an important role, e.g. synchrotron radiation, beam gas bremsstrahlung and availability of tunnel.

Another method to measure the polarization uses the well known effect[4,5] that if the electron and positron are transversely polarized then the $d\sigma/d\Omega$ of the $e^+e^- \rightarrow \mu^+\mu^-$, $\gamma\gamma$ and e^+e^- are modified showing a ϕ dependence that is a unique signature and measurement of the polarization of the initial state particles. This effect is maximum at $\theta = \frac{\pi}{2}$ and $\phi = \frac{\pi}{2}$, ϕ is the azimuthal angle and θ is the scattering angle. Following[4,5] we write for the $d\sigma/d\Omega$

$$\frac{d\sigma}{d\Omega}(e^+e^- \rightarrow e^+e^-) = \frac{r_0^2}{16\gamma^2}\left(\frac{3+\cos^2\theta}{1-\cos\theta}\right)^2 \cdot \left[1 + \frac{|\bar{P}_1|\cdot|\bar{P}_2|\sin^4\theta}{(3+\cos^2\theta)^2}(1-2\sin^2\varphi)\right]$$

$$\frac{d\sigma}{d\Omega}(e^+e^- \to \gamma\gamma) = \frac{r_0^2}{4\gamma^2(1-\beta_e^2\cos^2\theta)} \cdot$$

$$\cdot \left[1+\cos^2\theta + |\bar{P}_1|\cdot|\bar{P}_2|\sin^2\theta\cdot(1-2\sin^2\varphi)\right]$$

$$\frac{d\sigma}{d\Omega}(e^+e^- \to \mu^+\mu^-) = \frac{r_0^2}{16\gamma^2}\beta_\mu\left[2-\beta_\mu^2\sin^2\theta\cdot\left[1+|\bar{P}_1||\bar{P}_2|(2\sin^2\varphi-1)\right]\right]$$

$|P_1|$ and $|P_2|$ is the magnitude of the polarization, r_o is the classical electron radius, γ = (Beam Energy/m_e), and β_μ and β_e are the velocities of the muons and electrons.

In Figures 7, 8, 9, 10, 11, and 12 we show $\frac{d\sigma}{d\Omega}(\theta,\phi)$ for various values of the P_1, P_2. One can see that in the case of Bhabha scattering, the polarization effects are not pronounced. So a detector that can separate these final state would be a slow monitor but a very useful tool to establish the existence of polarization and cross calibrate a fast monitor.

References

1. F. W. Lipps and H. A. Tolhoek, Physics 20, 85 (1954), also ibid 20, 395 (1954).

2. C. Prescott, SLAC TN-731 (1973).

3. Addendum to Proposal SP-7 by the University of Pennsylvania-Wisconsin Group (1973).

4. V. N. Baier, XLVI International School of Physics Enrico Fermi (1969)

5. W. T. Ford, A. K. Mann, and T. Y. Ling, SLAC Report No. 158.

Figure Captions

1. Schematic diagram of the proposed experimental setup.

2. Rates, modulation and time required to measure polarization to 10% if one scattered the laser between two bending magnets in a standard cell.

3. Same as 2 but for the scattering taking place between two bending magnets in a matching cell.

4. Same as 2 but for the scattering taking place at the exit of Q1.

5. Same as 2 but for the scattering taking place in the drift section 50 m away from the interaction region.

6. Factor multiplying the time needed to measure the polarization to 10% as shown in Figures 2-5 (where zero background was assumed) vs. signal/noise.

7. Plot of $\frac{d\sigma}{d\Omega}$ vs. ϕ, at $\theta = 90^\circ$ for $e^+e^- \to \mu^+\mu^-$.

8. Plot of $\frac{d\sigma}{d\Omega}$ vs. θ, at $\phi = 90^\circ$ for $e^+e^- \to \mu^+\mu^-$.

9. Plot of $\frac{d\sigma}{d\Omega}$ vs. ϕ, at $\theta = 90^\circ$, for $e^+e^- \to \gamma\gamma$.

10. Plot of $\frac{d\sigma}{d\Omega}$ vs. θ, at $\phi = 90^\circ$, for $e^+e^- \to \gamma\gamma$.

11. Plot of $\frac{d\sigma}{d\Omega}$ vs. ϕ, at $\theta = 90$, for $e^+e^- \to e^+e^-$.

12. Plot of $\frac{d\sigma}{d\Omega}$ vs. θ, at $\phi = 90$, for $e^+e^- \to e^+e^-$.

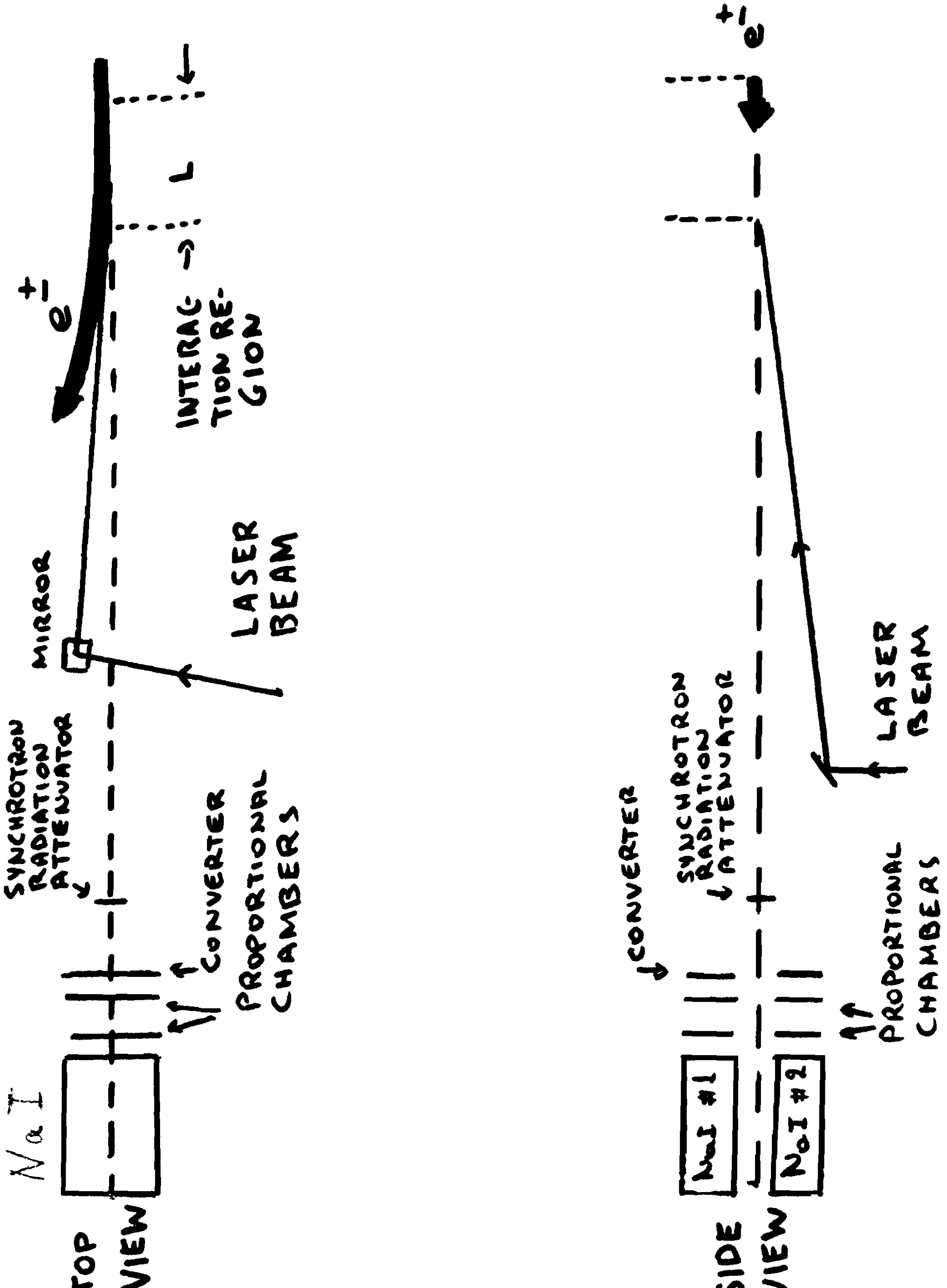
TOP VIEW
NaI
PROPORTIONAL CHAMBERS
CONVERTER
SYNCHROTRON RADIATION ATTENUATOR
MIRROR
LASER BEAM
INTERACTION REGION
L
$e^{\pm}$
SIDE VIEW
NaI #1
NaI #2
PROPORTIONAL CHAMBERS
CONVERTER
SYNCHROTRON RADIATION ATTENUATOR
LASER BEAM
$e^{\pm}$

FIG. 1

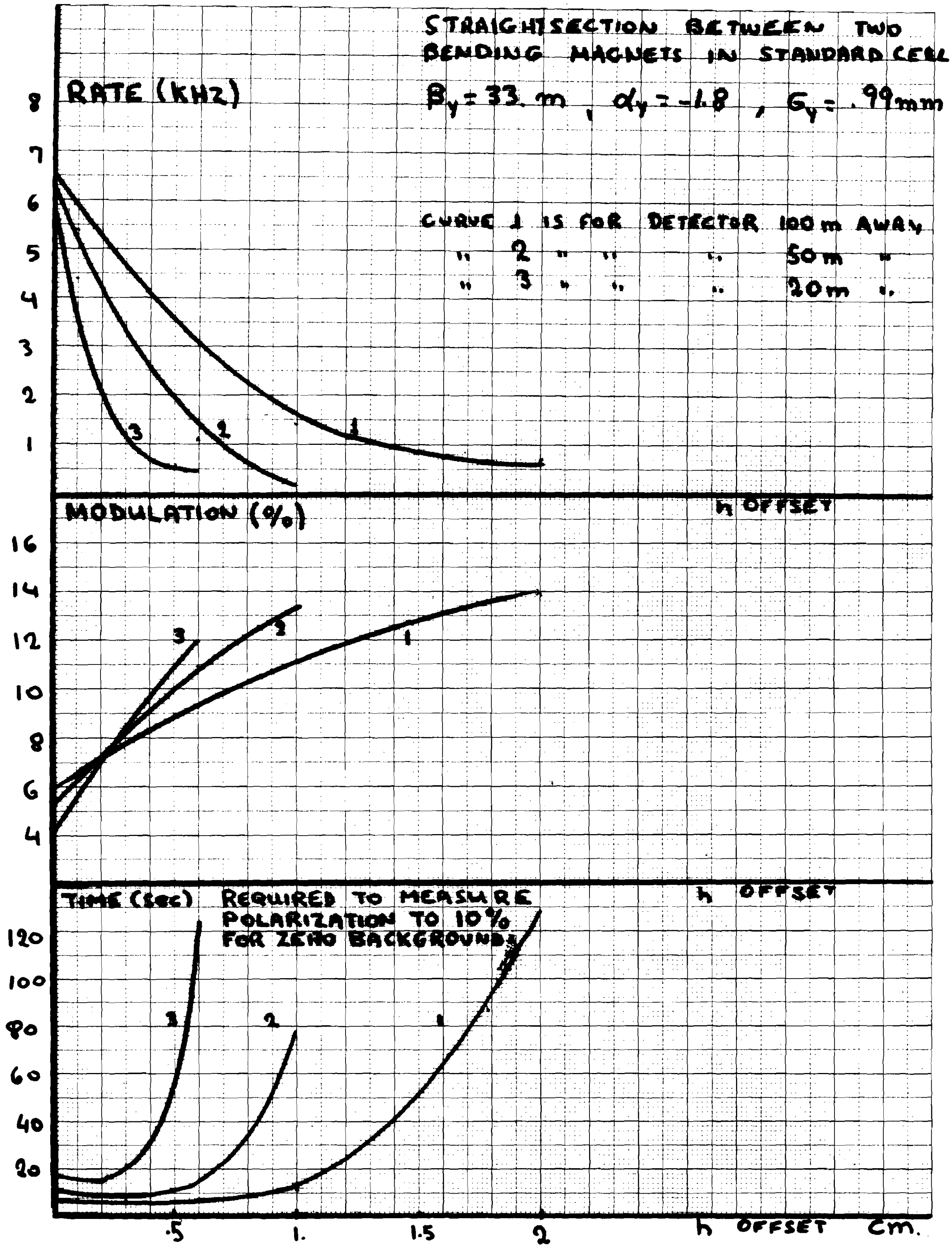
STRAIGHTSECTION BETWEEN TWO BENDING MAGNETS IN STANDARD CELL
$\beta_y = 33.\ m$, $\alpha_y = -1.8$, $\sigma_y = .99 mm$
CURVE 1 IS FOR DETECTOR 100 m AWAY
" 2 " " " 50 m "
" 3 " " " 20 m "
RATE (KHZ)
MODULATION (%)
TIME (sec) REQUIRED TO MEASURE POLARIZATION TO 10% FOR ZERO BACKGROUND
h OFFSET
h OFFSET
h OFFSET cm.
.5
1.
1.5
2

FIG. 2

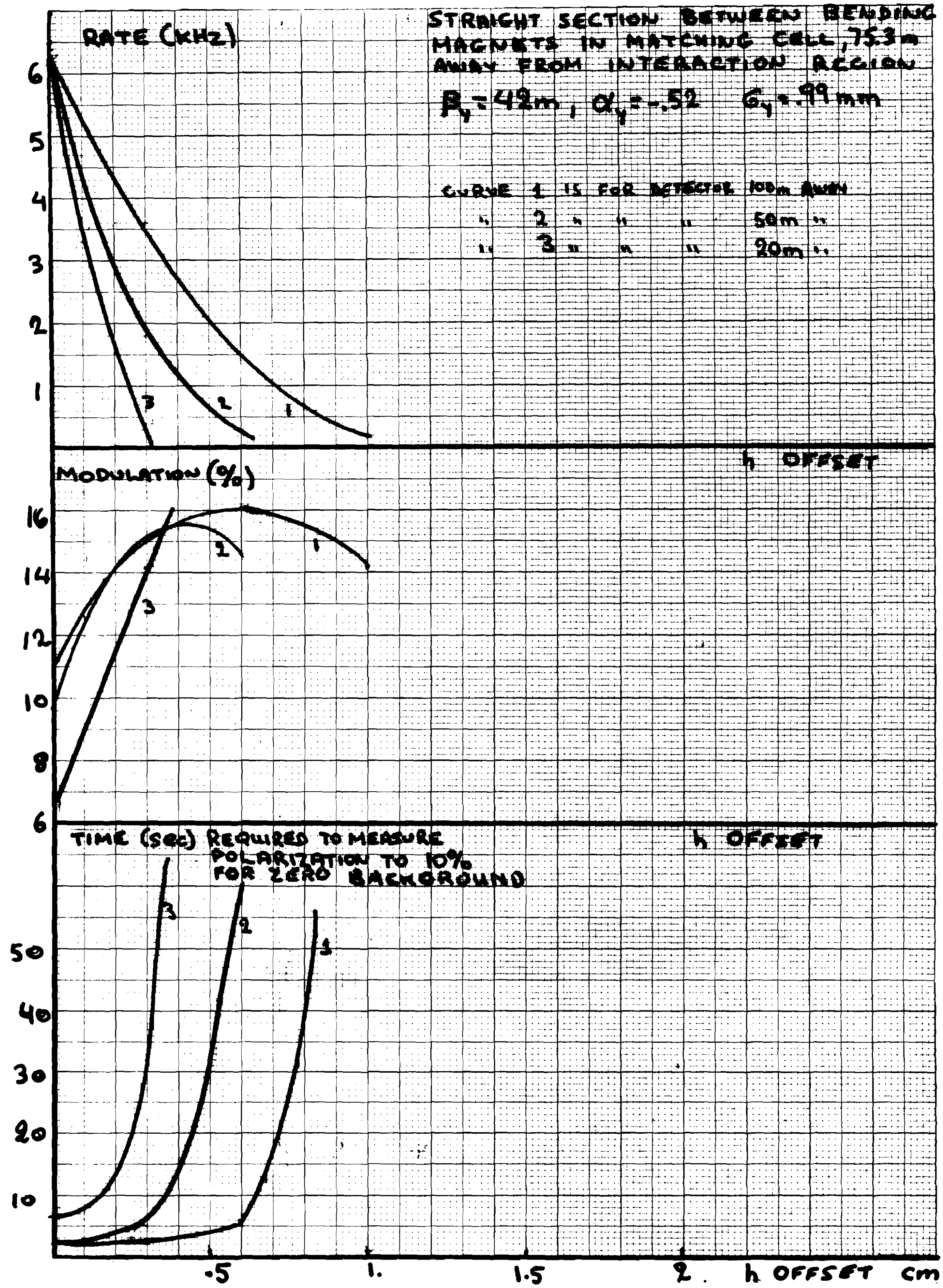
RATE (kHz)
STRAIGHT SECTION BETWEEN BENDING MAGNETS IN MATCHING CELL, 75.3m AWAY FROM INTERACTION REGION
$\beta_y = 42m$, $\alpha_y = -.52$ $\sigma_y = .99$ mm
CURVE 1 IS FOR DETECTOR 100m AWAY
" 2 " " " 50m "
" 3 " " " 20m "
h OFFSET
MODULATION (%)
h OFFSET
TIME (sec) REQUIRED TO MEASURE POLARIZATION TO 10% FOR ZERO BACKGROUND
h OFFSET cm
.5
1.
1.5
2.

FIG. 3

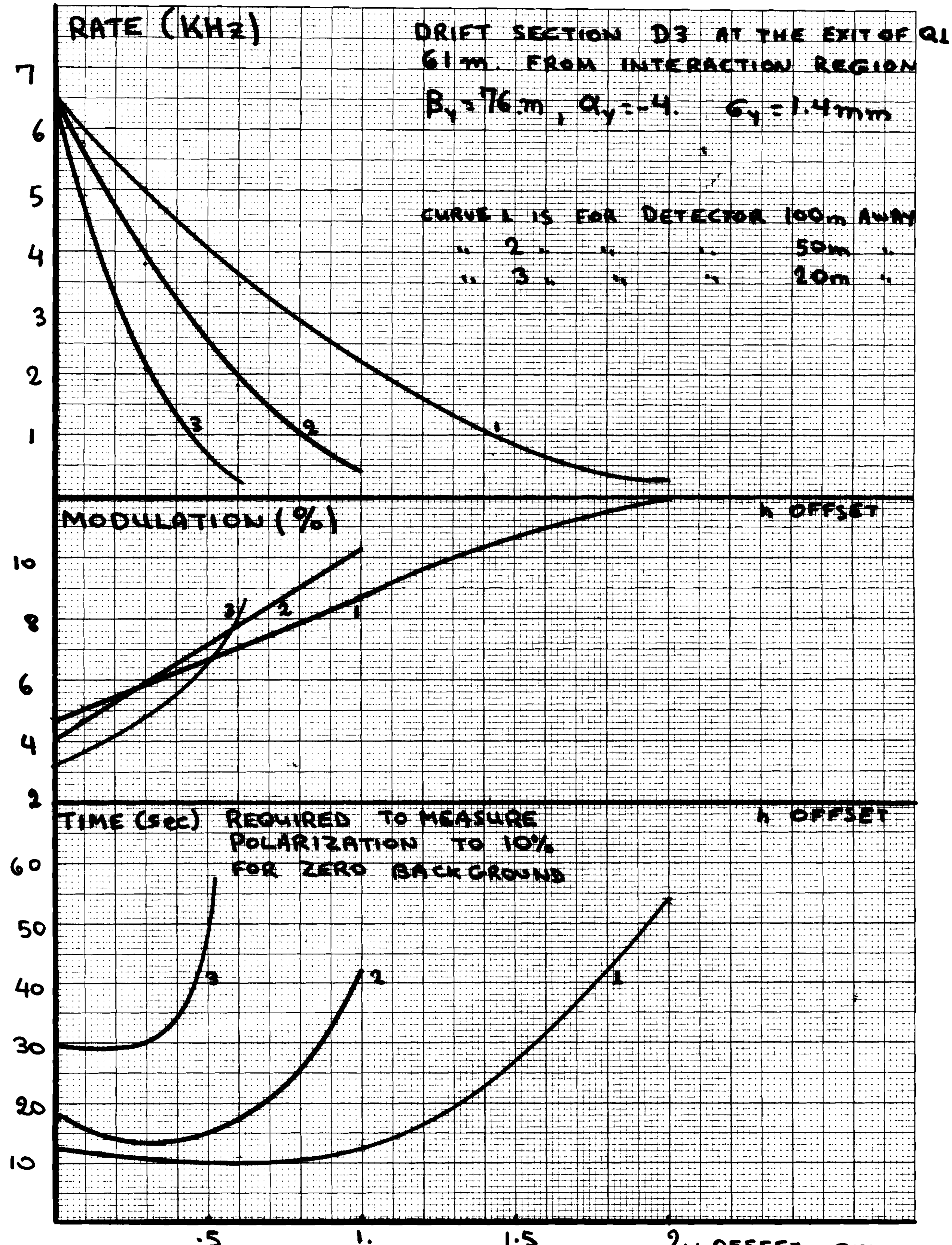
RATE (KHz)
DRIFT SECTION D3 AT THE EXIT OF Q1
61 m. FROM INTERACTION REGION
$\beta_y = 76\,m$, $\alpha_y = -4$. $\sigma_y = 1.4\,mm$
CURVE 1 IS FOR DETECTOR 100m AWAY
" 2 " " " 50m "
" 3 " " " 20m "
MODULATION (%)
h OFFSET
TIME (sec) REQUIRED TO MEASURE
POLARIZATION TO 10%
FOR ZERO BACKGROUND
h OFFSET
h OFFSET cm.

FIG 4

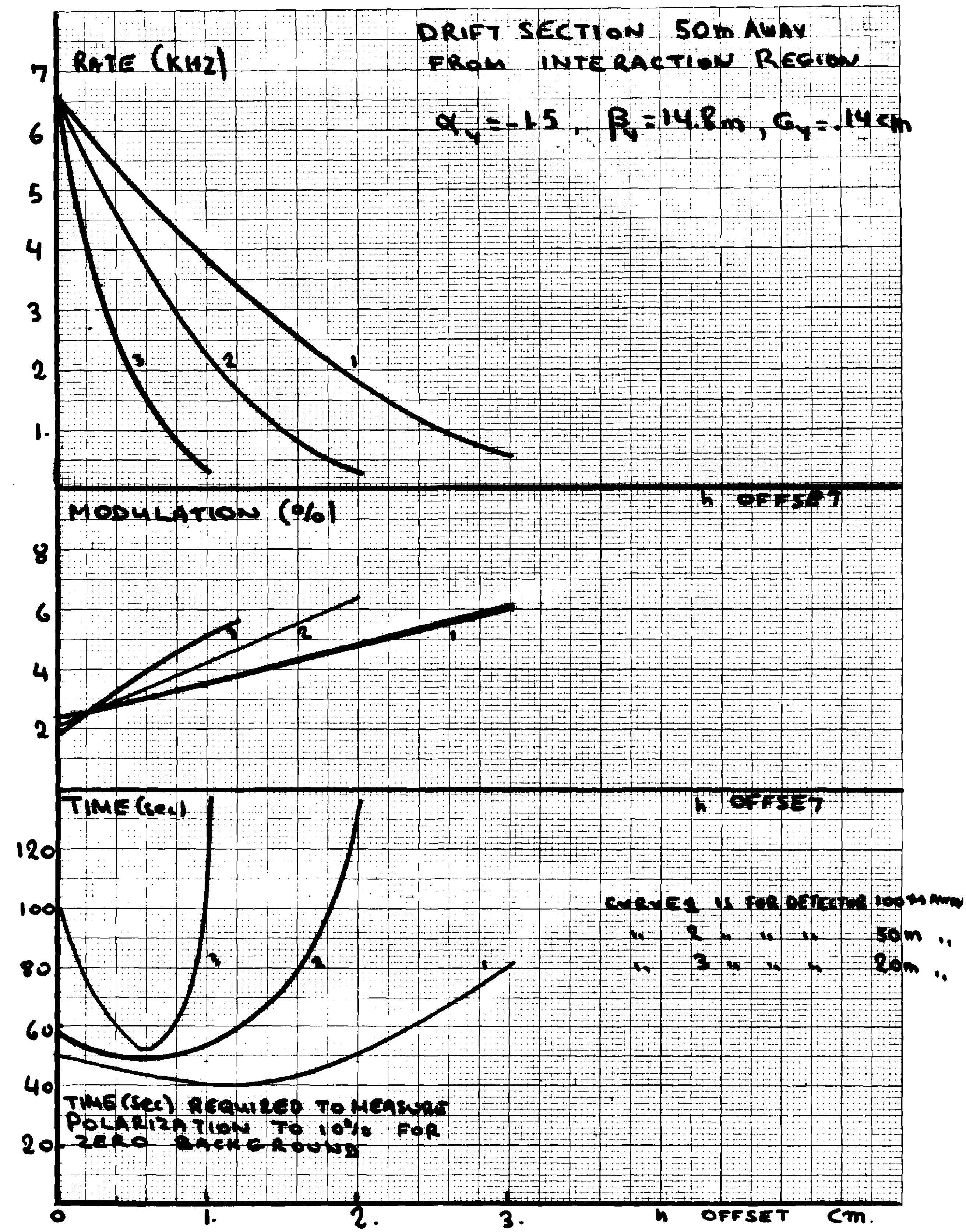
DRIFT SECTION 50m AWAY FROM INTERACTION REGION
$\alpha_y = -1.5$, $\beta_y = 14.8$m, $\sigma_y = .14$ cm
RATE (KHZ)
7
6
5
4
3
2
1.
3
2
1
h OFFSET
MODULATION (%)
8
6
4
2
h OFFSET
TIME (sec)
120
100
80
60
40
20
CURVE 1 IS FOR DETECTOR 100m AWAY
" 2 " " " 50m "
" 3 " " " 20m "
TIME (SEC) REQUIRED TO MEASURE POLARIZATION TO 10% FOR ZERO BACKGROUND
0
1.
2.
3.
h OFFSET Cm.

FIG. 5

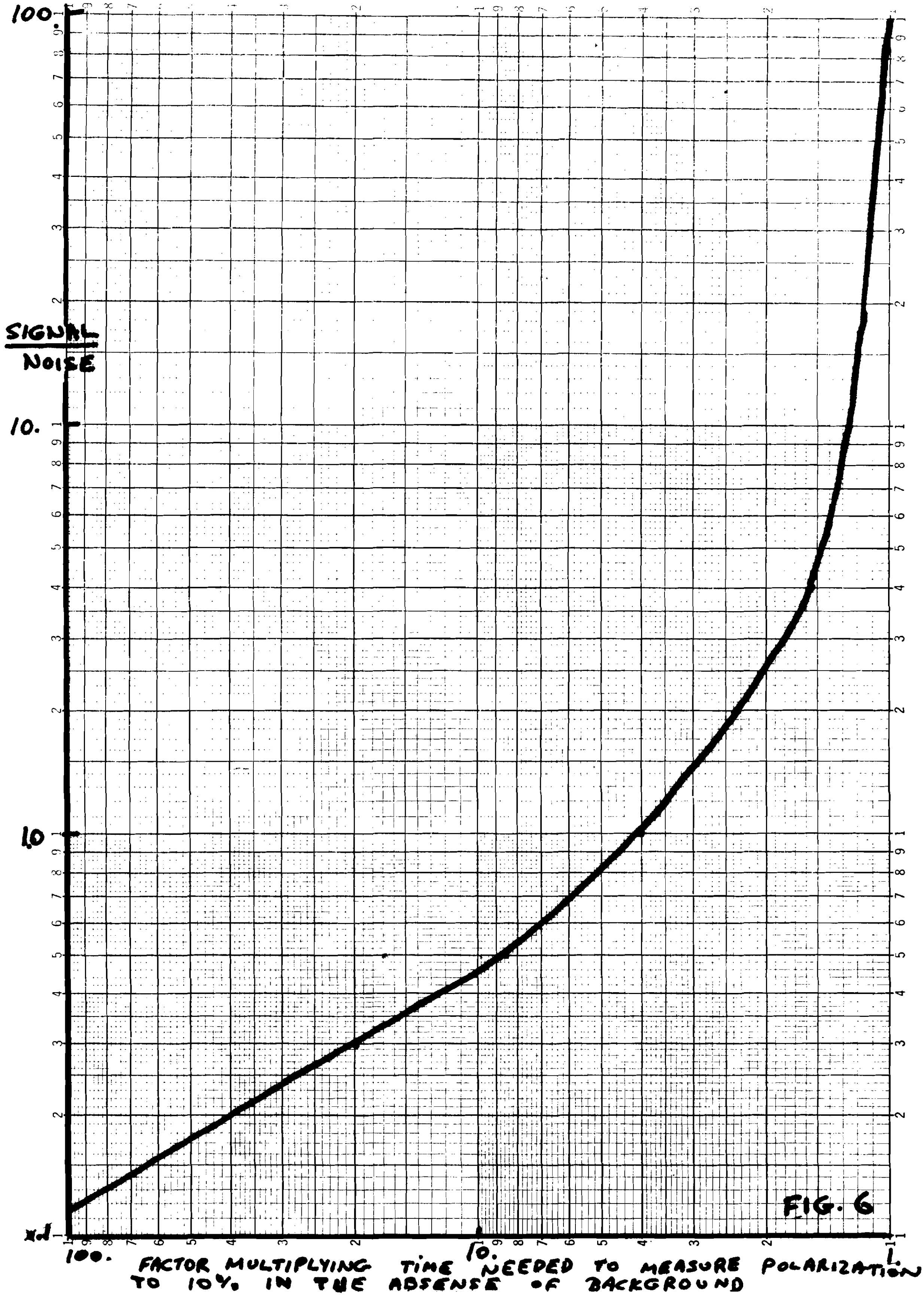
100.
SIGNAL
NOISE
10.
1.0
.1
100.
10.
1.
FACTOR MULTIPLYING TIME NEEDED TO MEASURE POLARIZATION TO 10% IN THE ABSENSE OF BACKGROUND

FIG. 6

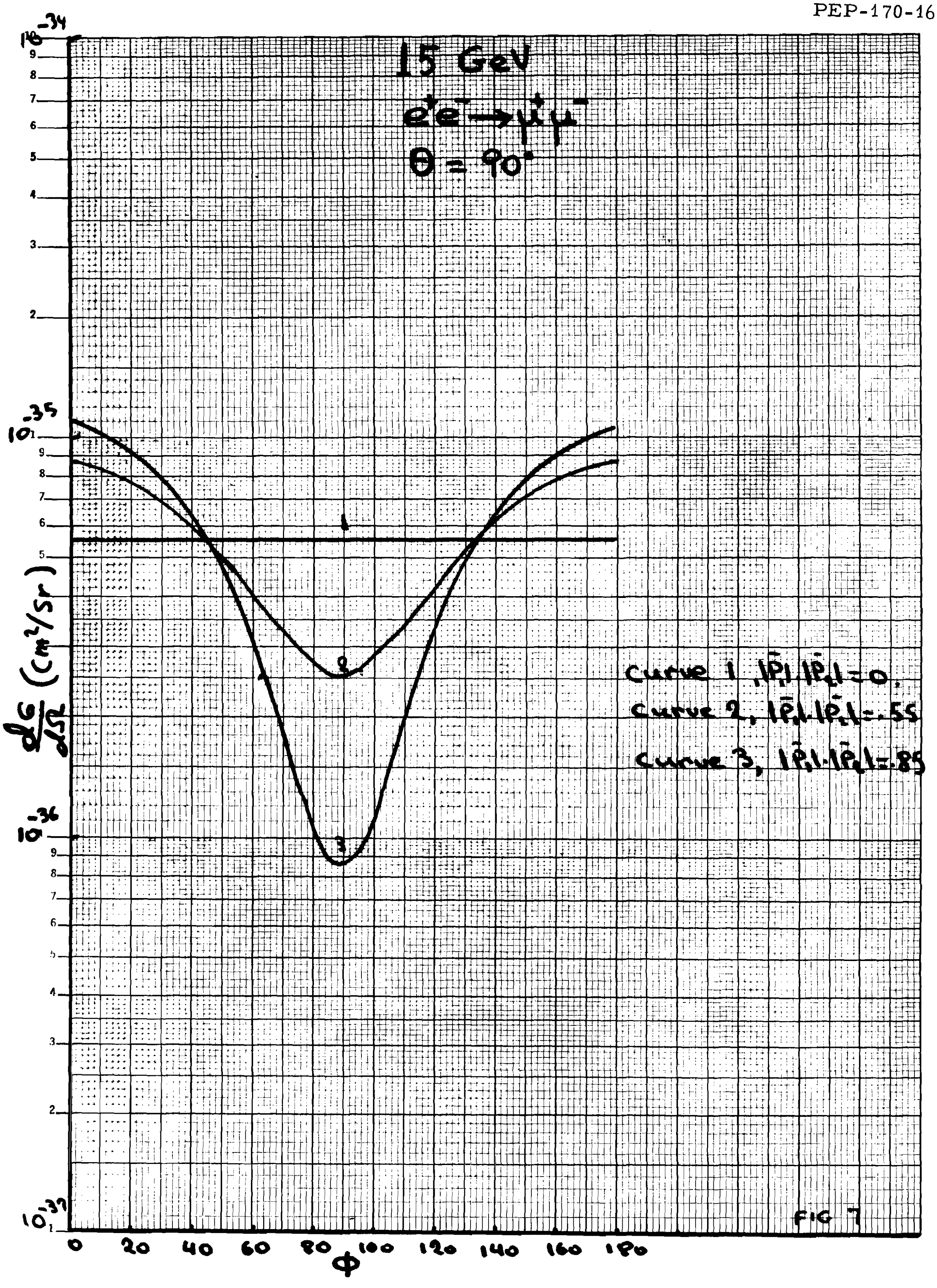

15 GeV
$e^+e^- \to \mu^+\mu^-$
$\theta = 90°$
10^{-34}
10^{-35}
10^{-36}
10^{-37}
$\frac{d\sigma}{d\Omega}$ (cm²/sr)
1
2
3
Curve 1, $|\bar{P}_1| \cdot |\bar{P}_2| = 0$.
Curve 2, $|\bar{P}_1| \cdot |\bar{P}_2| = .55$
Curve 3, $|\bar{P}_1| \cdot |\bar{P}_2| = .85$
0
20
40
60
80
100
120
140
160
180
ϕ

FIG 7

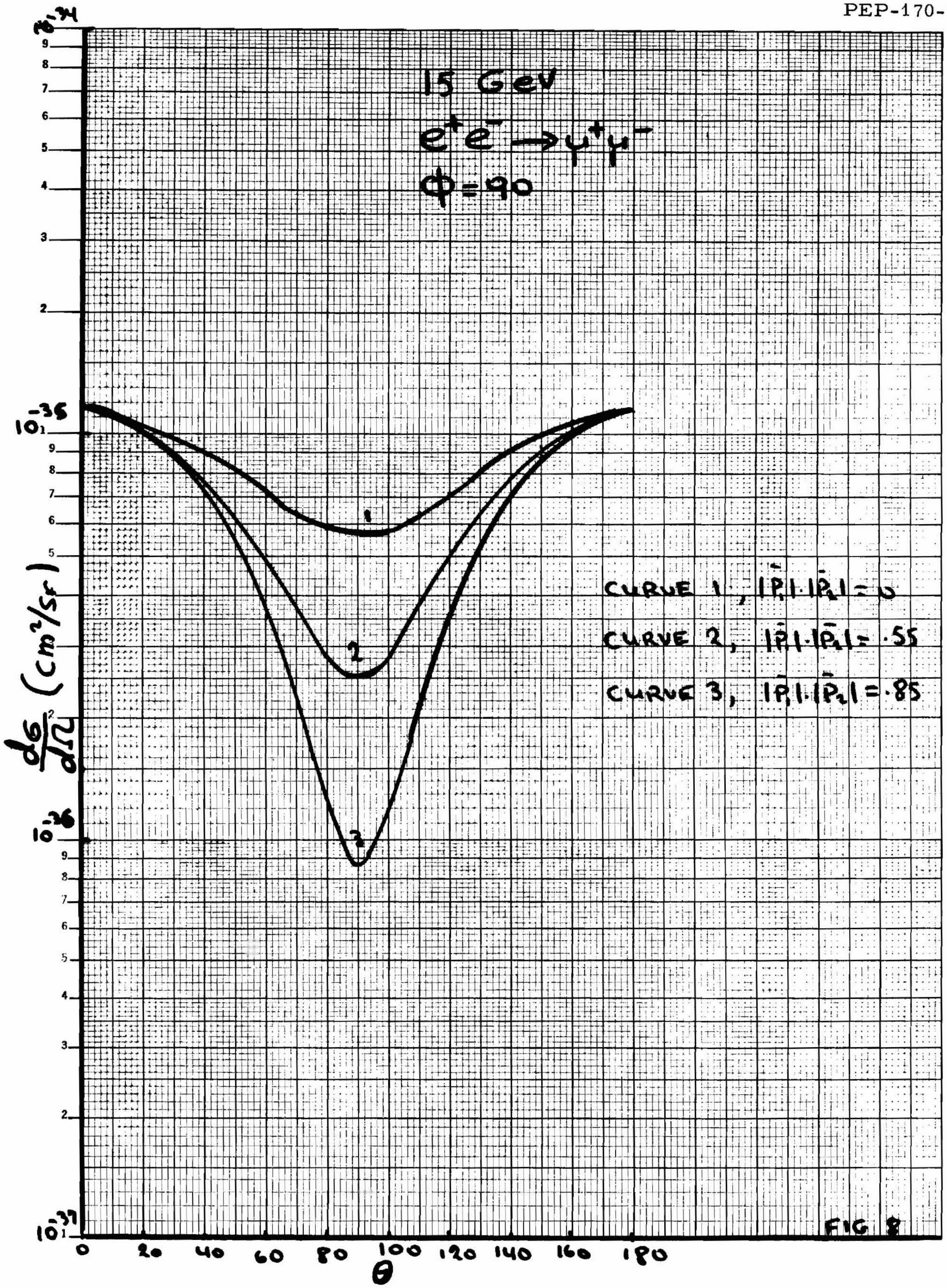
15 GeV
$e^+e^- \rightarrow \mu^+\mu^-$
$\phi = 90$
CURVE 1, $|\bar{P}_1| \cdot |\bar{P}_2| = 0$
CURVE 2, $|\bar{P}_1| \cdot |\bar{P}_2| = .55$
CURVE 3, $|\bar{P}_1| \cdot |\bar{P}_2| = .85$
$\frac{d\sigma}{d\Omega}$ (cm^2/sr)
10^{-34}
10^{-35}
10^{-36}
10^{-37}
θ
0
20
40
60
80
100
120
140
160
180

FIG 8

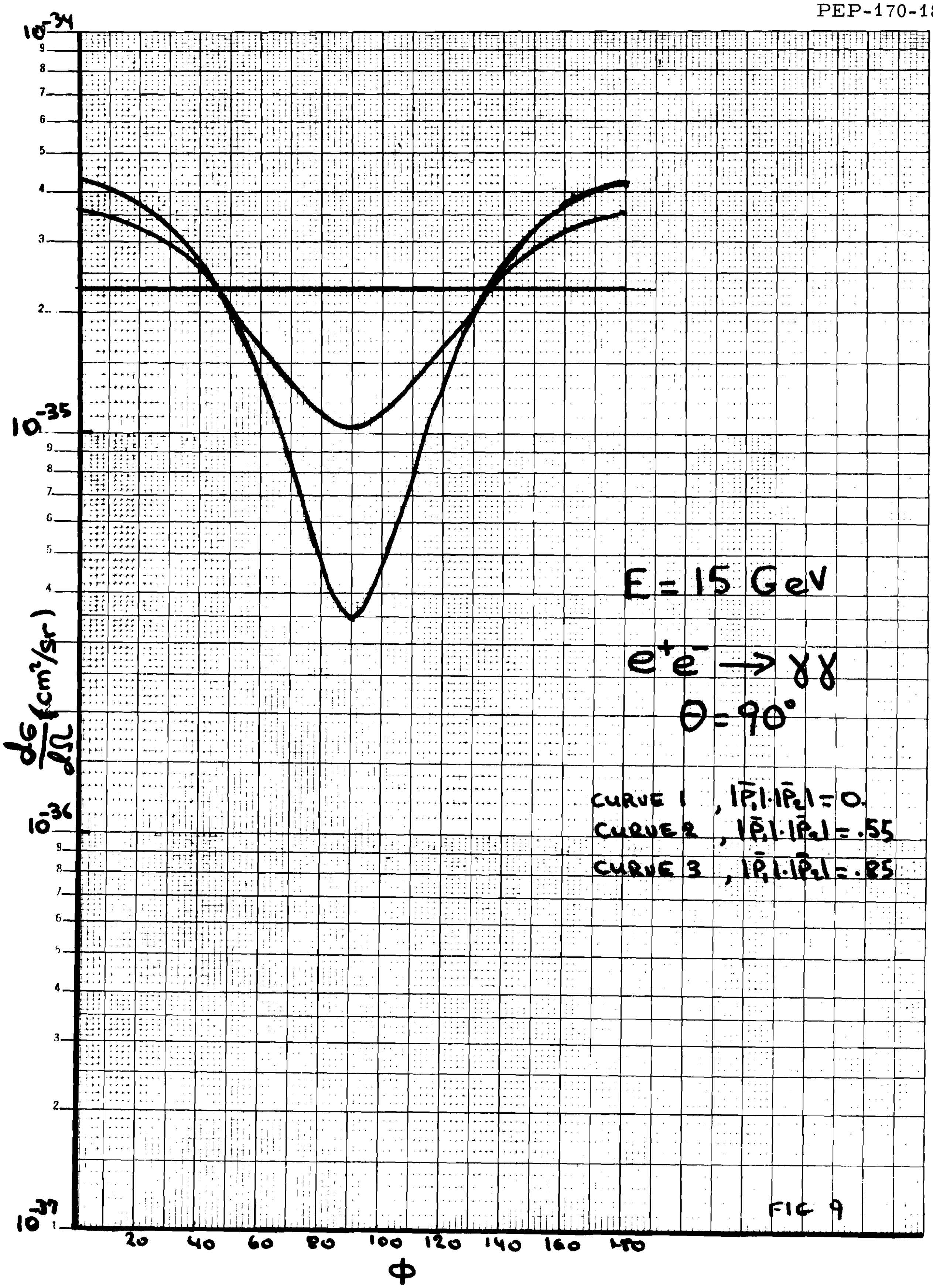
10^{-34}
10^{-35}
10^{-36}
10^{-37}
$\frac{d\sigma}{d\Omega}$ (cm²/sr)
20 40 60 80 100 120 140 160 180
ϕ
E = 15 GeV
$e^+e^- \to \gamma\gamma$
$\theta = 90°$
CURVE 1 , $|\bar{P}_1| \cdot |\bar{P}_2| = 0.$
CURVE 2 , $|\bar{P}_1| \cdot |\bar{P}_2| = .55$
CURVE 3 , $|\bar{P}_1| \cdot |\bar{P}_2| = .85$

FIG 9

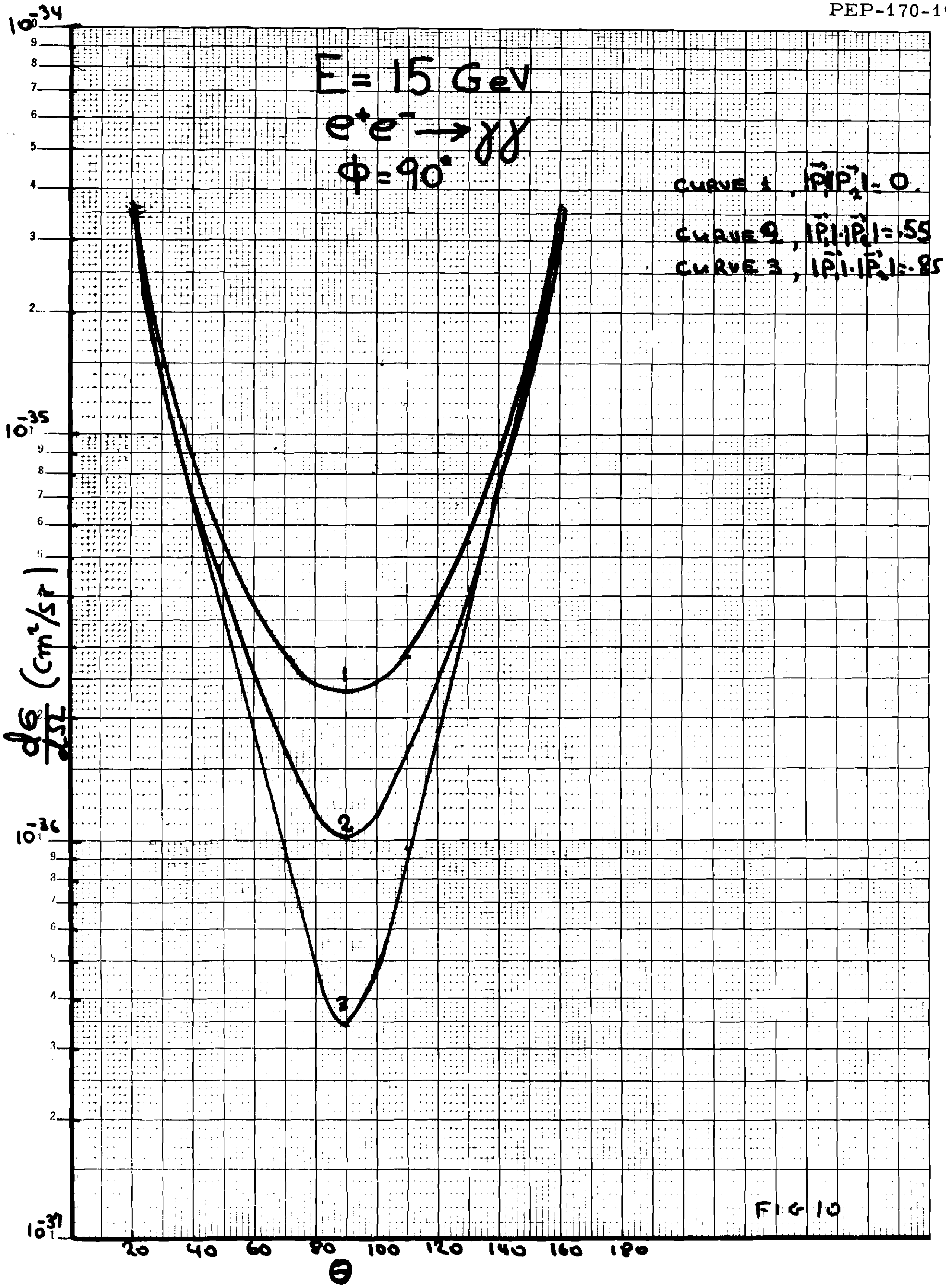
E= 15 GeV
$e^+e^- \rightarrow \gamma\gamma$
$\phi = 90°$
CURVE 1 , $|\vec{P}_1||\vec{P}_2| = 0$.
CURVE 2 , $|\vec{P}_1|\cdot|\vec{P}_2| = .55$
CURVE 3 , $|\vec{P}_1|\cdot|\vec{P}_2| = .85$
$\frac{d\sigma}{d\Omega}$ (cm²/sr)
10^{-34}
10^{-35}
10^{-36}
10^{-37}
20 40 60 80 100 120 140 160 180
θ
1
2
3

FIG 10

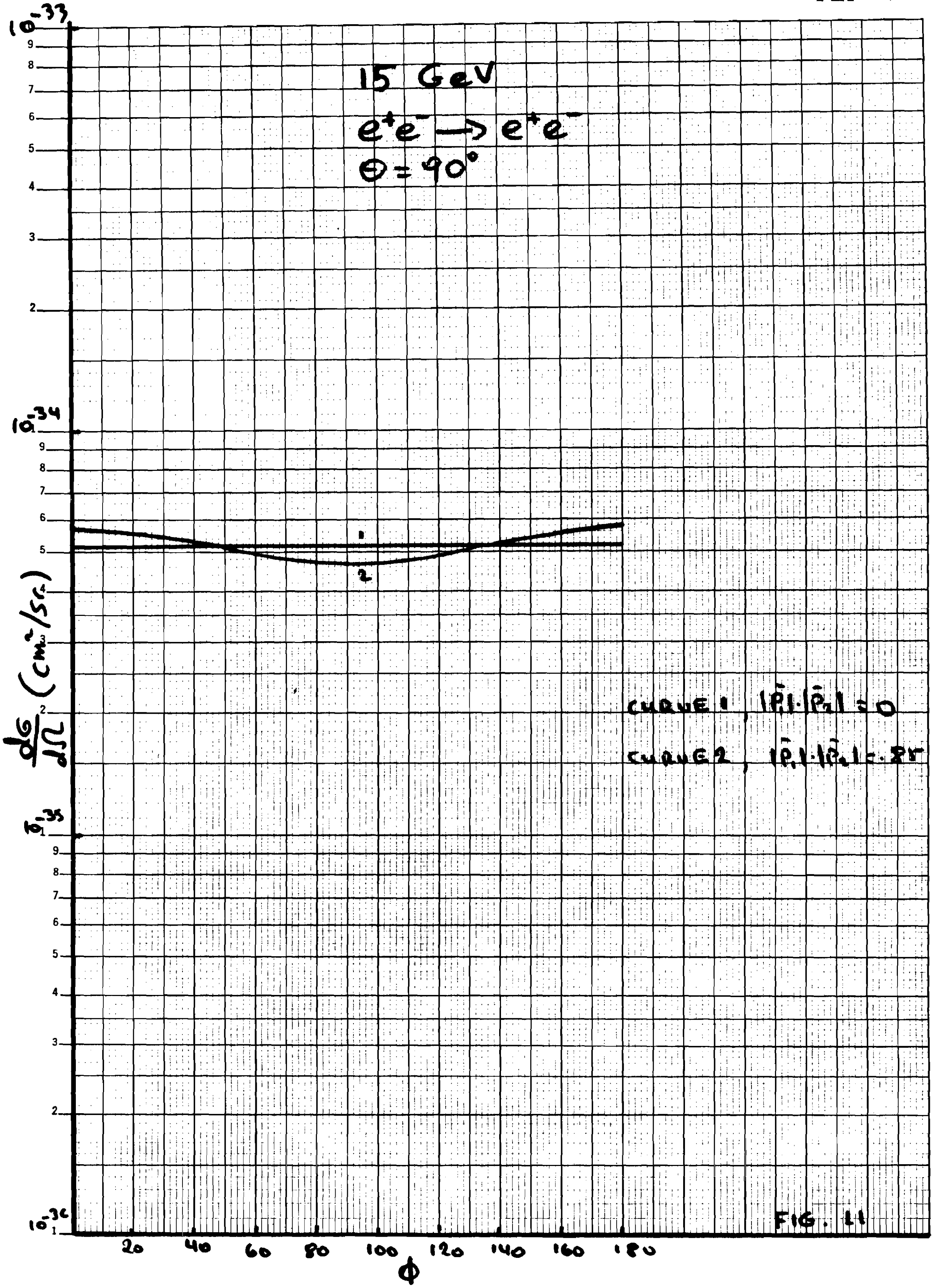
15 GeV
$e^+e^- \to e^+e^-$
$\Theta = 90°$
$\frac{d\sigma}{d\Omega}$ (cm²/sr)
CURVE 1, $|\vec{P}_1| \cdot |\vec{P}_2| = 0$
CURVE 2, $|\vec{P}_1| \cdot |\vec{P}_2| = .85$
ϕ
20 40 60 80 100 120 140 160 180

FIG. 11

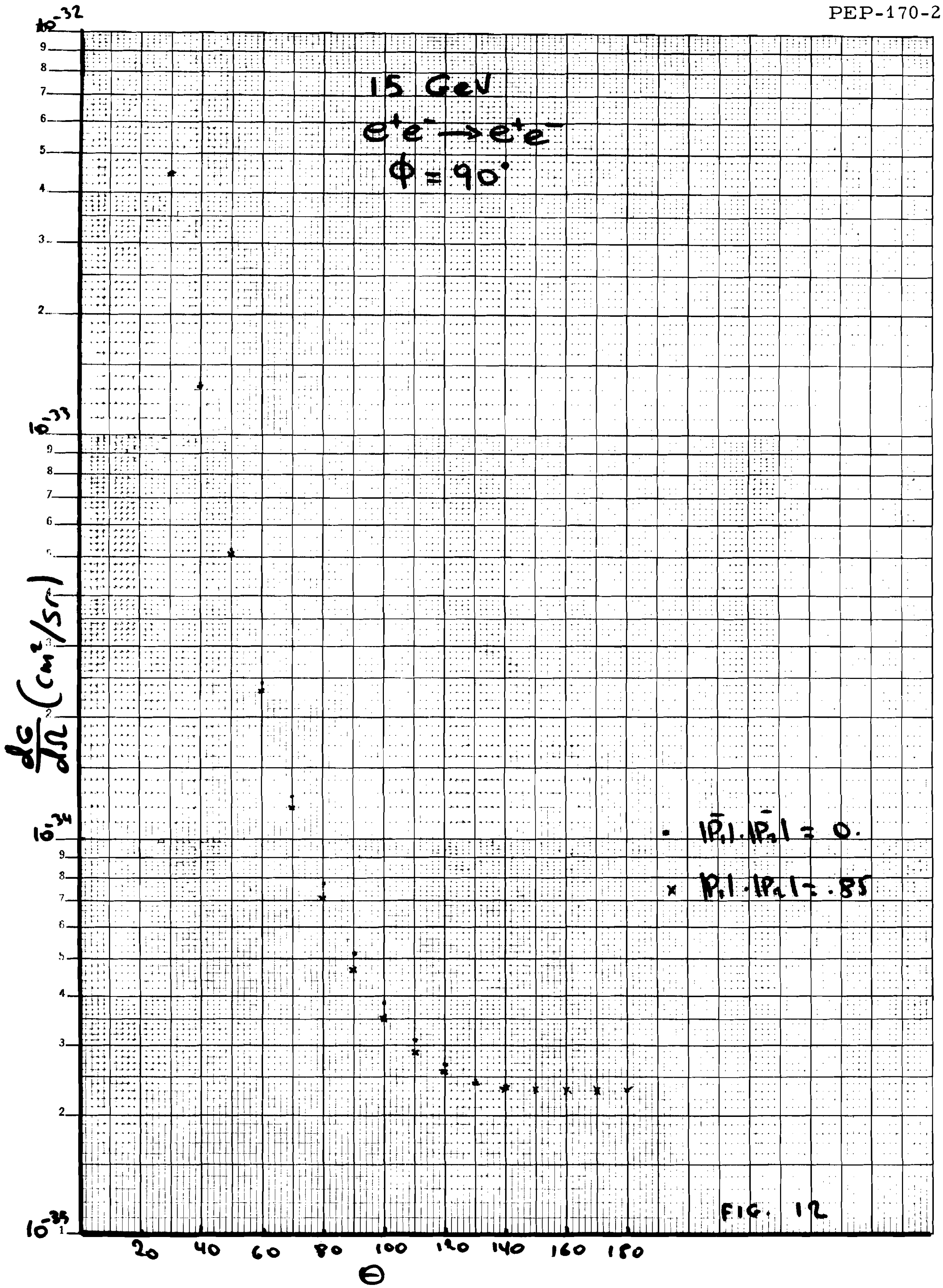
15 GeV
$e^+e^- \to e^+e^-$
$\phi = 90°$
$\frac{d\sigma}{d\Omega}$ (cm²/sr)
10^{-32}
10^{-33}
10^{-34}
10^{-35}
20 40 60 80 100 120 140 160 180
Θ
• $|\vec{P}_1|\cdot|\vec{P}_2| = 0.$
x $|P_1|\cdot|P_2| = .85$

FIG. 12